

Published in final edited form as:

Cereb Cortex. 2007 August ; 17(8): 1889. doi:10.1093/cercor/bhl097.

Mapping Cortical Thickness in Children with 22q11.2 Deletions

Carrie E. Bearden¹, Theo G.M. van Erp², Rebecca A. Dutton³, Helen Tran², Lara Zimmermann², Daqiang Sun², Jennifer A. Geaga³, Tony J. Simon⁴, David C. Glahn⁵, Tyrone D. Cannon^{1,2}, Beverly S. Emanuel⁶, Arthur W. Toga³, and Paul M. Thompson³

¹Department of Psychiatry and Biobehavioral Sciences, Semel Institute for Neuroscience and Human Behavior, University of California, Los Angeles, CA 90095, USA

²Department of Psychology, University of California, Los Angeles, CA 90095, USA

³Laboratory of Neuro Imaging and Brain Mapping Division, Department of Neurology, University of California, Los Angeles, CA 90095, USA

⁴Medical Investigations of Neurodevelopmental Disorders Institute, University of California, Davis, CA 95817, USA

⁵Department of Psychiatry, University of Texas Health Science Center at San Antonio, TX 78229, USA

⁶Division of Human Genetics of the Department of Pediatrics, The Children's Hospital of Philadelphia and University of Pennsylvania School of Medicine, Philadelphia, PA 19104, USA

Abstract

The 22q11.2 deletion syndrome (velocardiofacial/DiGeorge syndrome, 22q11.2DS) involves cardiac and craniofacial anomalies, marked deficits in visuospatial cognition, and elevated rates of psychosis. Although the mechanism is unknown, characteristic brain alterations may predispose to development of psychosis and cognitive deficits in 22q11.2DS. We applied cortical pattern matching and new methods for measuring cortical thickness in millimeters to structural magnetic resonance images of 21 children with confirmed 22q11.2 deletions and 13 demographically matched healthy comparison subjects. Thickness was mapped at 65 536 homologous points, based on 3-dimensional distance from the cortical gray-white matter interface to the external gray-cerebrospinal fluid boundary. A pattern of regionally specific cortical thinning was observed in superior parietal cortices and right parietooccipital cortex, regions critical for visuospatial processing, and bilaterally in the most inferior portion of the inferior frontal gyrus (pars orbitalis), a key area for language development. Several of the 30 genes encoded in the deleted segment are highly expressed in the developing brain and known to affect early neuronal migration. These brain maps reveal how haploinsufficiency for such genes can affect cortical development and suggest a possible underlying pathophysiology of the neurobehavioral phenotype.

Keywords

brain mapping; chromosome 22; genetics; MRI; velocardiofacial syndrome

© The Author 2006. Published by Oxford University Press. All rights reserved.

Address correspondence to Carrie E. Bearden, Department of Psychiatry and Biobehavioral Sciences, Semel Institute for Neuroscience and Human Behavior, University of California, Los Angeles, 300 Medical Plaza, Suite 2265, Los Angeles, CA 90095, USA. cbearden@mednet.ucla.edu.

Supplementary Materials

Supplementary materials can be found at <http://www.cercor.oxfordjournals.org/>.

Investigations of genetic mutations in mice have provided important insights into the molecular bases of memory and learning; however, molecular genetic approaches are only beginning to be utilized to advance the understanding of human cognition (Flint 1999). The 22q11.2 deletion syndrome (velocardiofacial/ DiGeorge syndrome, 22q11DS) results from a hemizygous deletion at chromosome 22q11.2. With an estimated prevalence of 1 out of 4000 live births, it is one of the most common genetic causes of intellectual disability (McDonald-McGinn et al. 1997). Physical manifestations of 22q11DS frequently include cleft palate, conotruncal heart defects, hypocalcemia, and facial dysmorphism (McDonald-McGinn et al. 1997). The cognitive phenotype includes early language delays and marked deficits in visuospatial cognition and arithmetic (Moss et al. 1999; Swillen et al. 1999; Bearden et al. 2001). We have previously identified a neurocognitive profile in this syndrome involving a selective deficit in memory for visuospatial locations (Bearden et al. 2001) (see Supplementary Fig. 1) and difficulty with spatial attentional orienting (Simon et al. 2005).

This syndrome is also associated with substantially elevated rates of psychopathology, particularly psychotic illness (Murphy 2002). At least 30 genes are encoded in the commonly deleted segment, several of which are highly expressed in the developing brain and known to affect early neuronal migration (Maynard et al. 2003). This syndrome therefore provides a useful model to investigate specific genetic influences on human cognitive function and brain development.

Prior studies using traditional volumetric approaches and voxel-based morphometry implicate abnormalities of posterior brain regions in 22q11DS (Eliez et al. 2000, 2001; Kates et al. 2001; van Amelsvoort et al. 2001; Bearden et al. 2004), as well as increased frequency of developmental midline anomalies (van Amelsvoort et al. 2001; Chow et al. 2002). In addition, Bingham et al. (1997) observed enlargement of the Sylvian fissures in infants with 22q11DS, suggesting delayed growth of the opercular region. Development of the operculum is one of the major expressions of the functional maturity of the brain and is embryologically related to the development of the face, as well as temporal lobe structures, critical for language development (Chen et al. 1996). Thus, it has been proposed that abnormal development of the operculum may explain some of the neurodevelopmental features associated with 22q11DS (Bingham et al. 1997).

Progress in understanding how this genetic deletion impacts brain structure and function is hindered by the absence of detailed maps establishing the scope and anatomical extent of brain anomalies in this syndrome. We therefore set out to create the first detailed cortical thickness maps in 22q11DS, using a novel method that creates group-average maps of gray matter (GM) thickness over the entire human cortex (Thompson et al. 2005). Cortical surface anatomy was carefully matched across individuals to provide spatially refined localizations of group differences relative to gyral landmarks over the cerebral surface. Based on prior imaging and neurocognitive studies in this syndrome, we predicted that areas in the parietal portion of the dorsal processing stream might show relatively greater cortical thinning than the adjacent perisylvian language regions. In addition, we anticipated finding increased cortical thinning in 22q11DS in the frontal opercular region (pars opercularis), consistent with delayed growth of this region.

Finally, given the hypothesized association between brain asymmetries and neurodevelopmental processes (e.g., Galaburda et al. 1978; Galaburda and Geschwind 1981; Harrison 1999), we wanted to also investigate whether abnormal cortical asymmetry may be a feature of 22q11DS. In particular, Crow (1990) has theorized that the mechanisms that determine asymmetrical brain development during neurodevelopment are closely linked to the disease process in schizophrenia and that schizophrenia may thus be linked to a defect of a gene controlling cerebral lateralization. Supporting this notion, some studies have found that

patients with schizophrenia show a loss of normal asymmetry in temporal lobe regions (Highley et al. 1999; McDonald et al. 2000). Thus, we mapped systematic asymmetries in cortical thickness, in order to determine whether 22q11DS is similarly associated with abnormal cortical asymmetry.

Materials and Methods

Subjects

Subject ascertainment procedures were identical to those reported in Bearden et al. (2004). Briefly, 22q11DS participants were recruited through the Clinical Genetics Department at the Children's Hospital of Philadelphia (CHOP); genetic diagnosis of 22q11.2 microdeletion was confirmed by fluorescence in situ hybridization studies with the N25 (D2S75) molecular probe from Oncor (Gaithersburg, MD). The CHOP Institutional Review Board approved the study, and signed informed assents and consents were obtained from all subjects and their parents, respectively. A total of 21 22q11DS patients and 13 normal comparison subjects participated in the study (see Table 1). Normal comparison subjects were recruited through advertisement in the hospital community and were matched with probands for race, handedness, parental social class, sex, and age (each subject was individually matched within 14 months). A minimum intelligence quotient (IQ) of 85 (1 SD below the population mean) and absence of previous neurological or psychiatric disorder were used as inclusion criteria for controls.

Magnetic Resonance Imaging Procedures

Acquisition—Magnetic resonance (MR) images of each subject's brain were acquired using a 1.5-T Siemens scanner in the Department of Radiology at CHOP. An average of 160 interleaved, 1-mm-thick transaxial slices were acquired using a conventional dual-spin echo sequence, with a repetition time of 2800 ms, echo times of 20 and 80 ms, a flip angle of 90°, and no interslice gap. The matrix size was 256 × 256 pixels, corresponding to a field of view of 23 cm and an in-plane resolution of 0.9 × 0.9 mm. Scans were analyzed at the University of California, Los Angeles, Laboratory of Neuro Imaging (LONI) by image analysts blinded to all subject information, including age, sex, and diagnosis. All MR images were processed with a series of manual and automated procedures detailed in other reports and summarized below. Cortical surface analyses were identical to those described in Thompson et al. (2003, 2004).

Anatomical Measurements

Image Processing—Image volumes passed through a number of preprocessing steps using mostly automated procedures implemented in the LONI Pipeline Processing Environment (Thompson et al. 2004). First, we created an intracranial mask of the brain using a brain surface extraction algorithm tool that is based on a combination of nonlinear smoothing, edge finding, and morphological processing (Shattuck and Leahy 2002). Any small errors in the masks were corrected manually to separate intracranial regions from surrounding extracranial tissue. Brain masks and anatomical images were corrected for head alignment and individual differences in brain size by using an automatic 9-parameter registration (Collins et al. 1994) to transform each brain volume into alignment with the target space and dimensions of the ICBM-305 reference brain created by the International Consortium for Brain Mapping (Mazziotta et al. 1995). Using the normalized brain masks, all extracerebral tissues were removed from the normalized image volumes. After applying radio frequency bias field corrections to eliminate intensity drifts due to magnetic field inhomogeneities, each image volume was segmented into different tissue types by classifying voxels based on their signal intensity values (Shattuck and Leahy 2002). Tissue classified brain volumes were resampled to 0.33-mm cubic voxels to improve the spatial resolution and precision of subsequent thickness measurements. Cortical thickness—defined as the 3-dimensional (3D) distance (in mm) between inner GM-white

matter (WM) border and the closest point on the outer surface (cerebrospinal fluid [CSF]-GM border)—was calculated using the Eikonal fire equation (Thompson et al. 2005) applied to voxels classified as GM. Cortical thickness was estimated voxel by voxel and projected as a local value (in mm) onto the cortical surface, where a smoothing kernel was used to average thickness measures within a 15-mm sphere at each cortical surface point, increasing signal-to-noise. These preprocessing steps are summarized and illustrated in Supplementary Figure 2.

Anatomical Analysis—An image analysis technique, known as cortical pattern matching (Thompson et al. 2003, 2004), was used to localize disease effects on cortical anatomy and increase the power to detect group differences. The approach models, and controls for, gyral pattern variations across subjects. Briefly, we created 3D cortical surface models based on automatically generated spherical mesh surfaces that were continuously deformed to fit a threshold intensity value that best differentiates extracortical CSF from the underlying cortical GM (MacDonald et al. 1994). As a result of the linear transformation procedure, the generated 3D cortical surface models correspond globally in size and orientation. Nevertheless, the same parameter space coordinates, within each cortical surface model, do not yet index the same anatomy across all subjects and across the left and right hemispheres (LH and RH, respectively). Therefore, the cortical surface models from each individual were used to identify and manually outline 16 sulci in each hemisphere, where image analysts (H.T. and L.Z.) were blind to subject diagnosis, sex, and age. The outlined lateral sulci included the Sylvian fissure; central, precentral, and postcentral sulci; superior temporal sulcus (STS) main body; STS ascending branch; STS posterior branch; primary and secondary intermediate sulci; inferior temporal; superior and inferior frontal; intraparietal; transverse occipital; olfactory; occipitotemporal; and collateral sulci. In addition to contouring the major sulci, a set of 6 midline landmark curves bordering the longitudinal fissure were outlined in each hemisphere to establish hemispheric gyral limits. Spatially registered gray-scale image volumes in coronal, axial, and sagittal planes were available simultaneously to help disambiguate brain anatomy. Landmarks were defined according to a detailed anatomical protocol (Sowell et al. 2001) based on the Ono sulcal atlas (Ono et al. 1990). These criteria, along with interrater reliability measures, have been described previously (Sowell et al. 2001), and the written anatomical protocol can be obtained via the Internet: http://www.loni.ucla.edu/~khayashi/Public/medial_surface/.

Statistical Analysis—We first calculated the mean thickness at each of the 65 536 cortical surface points across subjects and then generated statistical maps indicating group differences in local GM thickness. To do this, at each cortical point, a regression was run to assess whether the thickness of the cortical GM at that point depended on group membership. The *P* value describing the significance of this linkage was plotted on at each point on the cortex using a color code to produce a statistical map (e.g., Fig. 2). The statistical maps (uncorrected) are crucial for allowing us to visualize the spatial patterns of GM deficits, but permutation methods (Thompson et al. 2003) were used to assess the significance of the statistical maps and to correct for multiple comparisons. In each case, the covariate (group membership) was permuted 100 000 times on an SGI Reality Monster supercomputer with 32 internal R10000 processors, and a null distribution was developed for the area of the average cortex with group difference statistics above a fixed threshold in the significance maps. An algorithm was then developed to report the significance probability for the overall loss patterns in each map as a whole (Thompson et al. 2003), after the appropriate correction for multiple comparisons. In addition, based on our a priori hypotheses regarding specific brain regions that might be affected in 22q11DS, we conducted permutation tests in 2 specific regions of interest (ROIs), created for each individual from a probabilistic atlas (Evans et al. 1996) by transforming the probabilistic ROIs from standardized space back into the resliced space of each individual using an automated 9-parameter linear transformation (Collins et al. 1994), as described above. We

created one ROI for the ventral frontal lobe (ventral and dorsal regions separated by an axial plane passing through the intersection of the posterior extent of the inferior frontal sulcus and the precentral sulcus in each hemisphere) and one for the parietooccipital cortex. Anatomical criteria for these ROIs are detailed in previous publications (Ballmaier et al. 2004). The individual ROIs are then applied to the average surface map and used to define regions on it. The regions in each individual brain that are mapped into this ROI already correspond, due to the cortical pattern-matching methods employed. In the permutation analyses, subjects were randomly assigned to diagnostic groups for 100 000 new correlational analyses at each surface point in each ROI, and the number of significant results (i.e., GM thickness at any surface point that significantly differed between groups [22q11DS vs. control] at the threshold of $P = 0.01$) that occurred in the real group difference test was compared with the null distribution of significant results that occurred by chance.

Asymmetry Analysis—In order to examine asymmetries in each diagnostic group, cortical thickness maps were reflected in midsagittal plane ($x = 0$). Next, we calculated ratios between local LH and RH thickness values in order to provide asymmetry maps indicating local hemispheric differences by percentages. Dividing the average LH cortical thickness by the corresponding RH value (after sulcal pattern matching across hemispheres) generated a ratio map of percentage asymmetries. Values greater than 1 indicate that the RH had lower cortical thickness compared with the LH; values less than 1 indicate that the LH had lower cortical thickness compared with the RH. Paired t -tests were performed at each cortical surface point, maintaining the sign (i.e., direction) of the differences, to assess the local differences in cortical thickness between LH and RH, separately for 22q11DS patients and controls. Uncorrected 2-tailed probability values ($P < 0.01$) from these tests were mapped directly onto the average cortical surface model of each group, providing detailed and spatially accurate maps of hemispheric thickness asymmetries. However, given that t -tests were made at thousands of cortical surface points and adjacent data points are highly correlated, permutation testing (as described above) was again employed to safeguard against Type I error.

Results

Overall Volumetric Differences

To provide context for the cortical GM maps, the overall reductions in total GM and WM in patients with 22q11DS are shown in Figure 1. As evident in Figure 1a, 22q11DS children had significantly smaller overall GM volume (by 11.2%, $F_{1,32} = 15.41$, $P \leq 0.001$), but total WM volume was nonsignificantly reduced (by 4.6%, $F_{1,32} = 0.73$, $P = 0.40$). LH and RH GM volumes were significantly decreased, by 11.97% ($F_{1,32} = 17.33$, $P \leq 0.001$) and 12.70% ($F_{1,32} = 19.92$, $P \leq 0.001$), respectively. At the lobar level, the GM deficit was highly significant across all lobes (frontal: 11.6 %, parietal: 16.3%, temporal: 8.8%, occipital: 17.2%; Fig. 1b), although there was only a trend-level reduction in WM volumes in the occipital lobe in 22q11DS patients (by 10.2%, $P < 0.06$; Fig. 1c).

Cortical Thickness Maps

Average maps of cortical thickness are shown for the 22q11DS and control groups in Figure 2a,b. As evident in Figure 2a,b, there is remarkable similarity between the regional thickness patterns in the 2 groups, with the thinnest cortex in striatal regions and relatively thicker cortex in frontal and temporal lobe regions, particularly the region surrounding the most anterior portion of the Sylvian fissure. Patients with 22q11DS showed 2 major anatomical regions of highly significant cortical thinning: 1) in a localized anatomical region encompassing the parietooccipital cortex and occipital poles and 2) in the most inferior portion of the inferior frontal gyrus (IFG) (pars orbitalis) and lateral orbital gyrus. Effects of greatest magnitude were found in the right parietooccipital cortex (red colors, Fig. 1c, left panel), where GM thickness

was 14% or more below the control average. In particular, a greater than 14% reduction in cortical thickness was observed in an area encompassing the right lateral occipital gyrus (Brodmann areas [BAs] 18 and 19, which comprise the visual association cortex). This region of significantly thinner cortex also includes the angular gyrus, a region that is critical for numerical cognition and heavily dependent on spatial representations (Hubbard et al. 2005). Similar to the pattern of cognitive deficits seen in 22q11DS, patients with lesions to this region frequently show visuoconstructive deficits and/or acalculia (Cohen et al. 2000). Cortical thinning in the LH was of lesser magnitude, and somewhat more anterior, encompassing portions of the angular and supramarginal gyri and posterior temporal lobe, including the middle and inferior temporal gyrus (BAs 21 and 37). No significant increases in thickness compared with controls were observed in any cortical location. We also compared the mean difference in thickness with a pointwise estimate of the standard error in cortical thickness to measure the significance of the thickness decreases (Fig. 2*d*). Correcting for multiple comparisons, both the RH and LH decreases were highly significant (respectively, $P = 0.025$ and $P = 0.0075$, corrected). These differences were also significant after multiple comparisons correction when a parietooccipital ROI was specifically examined (right: $P = 0.005$ and left: $P = 0.018$, corrected). A trend toward increased cortical thinning was observed in the right ventral frontal cortex ROI in 22q11DS ($P = 0.073$, corrected), but this difference was not significant in left ventral frontal cortex ($P = 0.12$, corrected).

Asymmetry Effects

Figure 3 displays the average distribution of local hemispheric differences in cortical thickness as a percent difference, for control participants and 22q11DS (Fig. 3*a*). Statistically significant asymmetries of cortical thickness are displayed in Figure 3*b* for normal controls (left panel) and for 22q11DS (right panel). Permutation tests were significant for the comparison of thickness between LH and RH for both controls ($P = 0.02$) and 22q11DS ($P = 0.007$), indicating that the observed asymmetry effects do not occur by chance. Rightward ($R > L$) asymmetries of cortical thickness were of greatest magnitude in the IFG (comprising the pars orbitalis, triangularis, and opercularis) in both 22q11DS and control children but were more pervasive in the brains of 22q11DS participants, extending into the anterior tip of the temporal lobe (Fig. 3*a,b*, right panel). In the control participants, regions of rightward asymmetry ($R > L$) were also observed in the posterior inferior temporal-occipital cortex, indicating that the cortex was approximately 5% thicker in the RH in these regions (Fig. 3*a*, left); in contrast, rightward asymmetry was seen more anteriorly in the 22q11DS participants, in the superior temporal gyrus and angular gyrus (BA 39; Fig. 3*a*, right). In controls, the most prominent regions of leftward asymmetry ($L > R$) were located in the anterior temporal lobe; in contrast, 22q11DS subjects showed a different pattern of $L > R$ asymmetry in inferior parietooccipital cortex (Fig. 3*b*).

Although statistical maps in Figure 3*b* appear to indicate group differences in cortical thickness asymmetry in the ventral frontal cortex, supplementary statistical analyses indicated a statistically significant regional interaction between group (22q11DS vs. control) and hemisphere only in the parietooccipital cortex ROI ($P = 0.02$; Supplementary Fig. 3).

Effects of Age

There was a moderate negative correlation between age and cortical thickness in the overall sample ($r = -0.37$, $P = 0.03$), which was of similar magnitude in the 22q11DS ($r = -0.39$, $P = 0.05$) and control groups ($r = -0.27$, $P = 0.08$). To further examine the effects of age on group differences in cortical thickness, we reanalyzed our group comparisons using analysis of covariance controlling for age. After covarying for age, results of diagnosis remained significant ($F_{2,31} = 12.36$, $P < 0.001$). Age was also a significant predictor in the model

($F_{2,31} = 32.84, P < 0.001$), indicating that age and diagnosis both exerted significant independent effects on cortical thickness.

Effects of Psychiatric Diagnosis

Psychiatric diagnoses within the 22q11DS patient group are presented in Table 1. No differences in cortical thickness were observed between 22q11DS patients with ($N = 9, 43\%$) and without ($N = 12, 57\%$) psychiatric diagnoses overall ($P \geq 0.40$ for both hemispheres).

Effects of Other Confounding Variables

Given the IQ differences between the patient and control groups, we examined the relationship of full-scale IQ with cortical thickness and found a slight, nonsignificant positive relationship in the overall sample ($r = 0.17, P = 0.30$). Correlations were similar in the patient and control groups ($r = 0.17, P = 0.50$; $r = 0.10, P = 0.70$, respectively).

In addition, we examined differences in cortical thickness as a function of history of cardiac surgery as this could potentially be a major source of environmentally caused neuroanatomical alteration in 22q11DS (Simon et al. 2002). Consistent with other samples of patients with this syndrome (e.g., Moss et al. 1999; Minier et al. 2005), 71% of our sample had a cardiac defect, most commonly ventroseptal defect, which was present in 43% of the total sample ($N = 9$). We found no differences in cortical thickness between 22q11DS patients with ($N = 15$) and without ($N = 6$) a cardiac defect ($F_{1,20} = 0.29, P = 0.59$).

Discussion

Here we visualized for the first time the profile of cortical anomalies associated with the genetic deletion in 22q11DS. Cortical thickness was significantly decreased (by 10–15%) in localized anatomical regions encompassing parietal and lateral occipital cortices, areas critical for visuospatial information processing. These regions, particularly in the RH, process spatial information and are critical for directing spatial attention, cognitive areas of disproportionate deficit in patients with 22q11DS. These results are quite consistent with prior anatomical parcellations that suggested disproportionately smaller parietal and occipital lobes and suggest that reduction in thickness of the cortical mantle may underlie the observed volumetric deficits (Eliez et al. 2000; Kates et al. 2001).

We also identified a localized decrease in cortical thickness in the pars orbitalis region of the IFG. Functional neuroimaging studies have found that this region (corresponding to BA 47, in the LH) is selectively involved in processing the semantic aspects of a sentence (Dapretto and Bookheimer 1999), and Lu et al. (2006) recently found that GM thickening in IFG was associated with developmental improvement in phonological processing abilities. Although patients with 22q11DS have a relative strength in verbal as compared with visuospatial memory, virtually all patients with this syndrome have early language delays, and language comprehension remains an area of relative weakness (Gerdes et al. 1999; Woodin et al. 2001). This region is slightly anterior to the frontal region in which we had anticipated finding increased cortical thinning in 22q11DS, the pars opercularis, based on prior findings of enlarged Sylvian fissures in infants with 22q11DS (Bingham et al. 1997). However, given the close proximity of these brain regions, it is possible that this localized area of cortical thinning may be related to abnormal prenatal development of perisylvian cortex. Interestingly, the infants studied in Bingham et al. (1997) consistently had disproportionate enlargement of the left Sylvian fissure compared with the right, suggesting lateralized effects of a gene or genes in the deleted region on the development of perisylvian cortex. Although specific genes known to be responsible for lateralization defects have not been yet mapped to the 22q11.2 region, the abnormal asymmetry of cortical thickness detected specifically in the parietooccipital

region in 22q11DS patients suggests that certain of the deleted genes may directly contribute to lateralization processes in the normal human cortex (Sun et al. 2005). Although here we detected significantly altered cortical asymmetry only in the parietooccipital ROI and not in frontal cortex, the observed cortical asymmetries in both regions warrant further investigation in future larger studies.

Although, to our knowledge, asymmetries of thickness have not previously been investigated across the cortical surface in normal children, Luders et al. (2006) used these same methods to investigate hemispheric asymmetries of cortical thickness and the influence of gender in young, healthy adults (mean age ~25 years). They found a similar asymmetry profile in both sexes, with more pronounced leftward than rightward asymmetry in the anterior temporal lobe, the precentral gyrus, and middle frontal regions. We found a very similar pattern of increased rightward asymmetry in the IFG and the inferior posterior temporal lobe. Thus, whereas leftward asymmetries appeared more pronounced in the older sample studied by Luders et al. (2006), the specific regions in which asymmetry was detected were quite similar in our study, particularly in the RH. In addition, using volumetric measures in normal children and adolescents aged 5–17 years, Reiss et al. (1996) previously reported a pattern of cerebral asymmetry involving rightward prominence of cortical GM, similar to the pattern we observed here using cortical thickness measures.

Notably, this cognitive profile of relative strengths in verbal memory, in contrast to marked deficits in visuospatial memory, bears striking similarity to that seen in another genetic deletion syndrome, Williams syndrome (WS; Bearden et al. 2002). However, unlike WS, there is no evidence that patients with 22q11DS are hypersociable or show particular strengths in musical ability (Karmiloff-Smith et al. 2004). Using identical methods to those reported here, a pattern of anatomically localized failure of cortical maturation was observed in patients with WS, involving a delimited zone of RH perisylvian cortex that was 5–10% thicker in WS than in matched controls, despite pervasive GM and WM deficits, but with corresponding deficits in adjacent dorsal stream regions including superior parietal areas (Thompson et al. 2005; see Supplementary Fig. 4). In addition, using functional brain imaging to assess task-related activation in WS, Meyer-Lindenberg et al. (2004) identified a pattern of hypoactivation in the parietal portion of the dorsal stream, concomitant with GM volume reduction in the immediately adjacent parietooccipital/intraparietal sulcus. A similar pattern of localized neuroanatomical deficits may underlie the visuospatial cognitive impairments characteristic of both 22q11DS and WS.

Relationship to Psychiatric Disorders

These cortical anomalies do not closely resemble those seen in schizophrenia, where prefrontal and temporal regions show greatest GM deficits (Wright et al. 2000). Developmental factors may play an important role in these differences. Using identical cortical pattern-matching methods to those reported here, Thompson et al. (2001) mapped cortical changes over time in adolescents with childhood onset of schizophrenia. Early deficits in parietal brain regions progressed anteriorly into temporal lobes, engulfing sensorimotor and dorsolateral prefrontal cortices over a 5-year period. Only the latest changes included dorsolateral prefrontal cortex and superior temporal gyri, deficit regions found consistently in adult studies, suggesting that these structural changes occur later in the course of illness. In this sample of children and adolescents with the deletion, we did not find evidence for differences in patterns of cortical thickness between patients with and without psychiatric disorders. However, only one patient had a psychotic disorder diagnosis; the majority had anxiety disorder and attention deficit hyperactivity disorder diagnoses, which are likely to be associated with more subtle neuroanatomical alterations (Milham et al. 2005) that may not result in detectable differences beyond those associated with the genetic deletion itself.

Effects of Development and IQ

Here we find a moderate inverse relationship between age and cortical thickness, in both patients with 22q11DS and healthy controls. After covarying for age, results of diagnosis remained significant. Thus, although developmental factors are clearly important, it does not appear that the slight, nonsignificant age difference between the groups accounts for the observed group differences in cortical thickness.

Consistent with the pattern seen in our healthy comparison subjects, O'Donnell et al. (2005) specifically examined changes in cortical thickness in the frontopolar cortex (FPC) through late childhood and adolescence and found a linear decline in cortical thickness in the FPC and the dorsolateral prefrontal cortex between the ages of 8 and 19 years.

Although measures of cortical thickness are fairly novel, earlier studies have examined changes in GM density over the course of development (a measure which is highly correlated with cortical thickness; Thompson et al. 2005). Studies of GM maturation indicate loss of cortical GM density over time, which is temporally associated with postmortem findings of increased synaptic pruning during adolescence and early adulthood (Sowell et al. 1999). In a longitudinal study examining the sequence of cortical GM development between the age of 4 and 21 years, Gogtay et al. (2004) found that primary sensorimotor cortices, along with frontal and occipital poles, mature first and the remainder of the cortex develops in a parietal-to-frontal (back-to-front) direction. Thus, alterations in either the degree or timing of basic maturational processes may at least partially underlie the pattern of cortical thickness deficit observed here.

Only one study has examined adults with 22q11DS using quantitative methods (van Amelsvoort et al. 2001). Compared with IQ-matched controls, adult patients demonstrated diffuse WM deficits in frontal regions, the fasciculus longitudinalis and optic radiation, and regionally specific GM reductions in the left cerebellum, insula, and frontal and right temporal lobes, suggesting that cerebellar anomalies may be relatively stable but additional frontal and temporal GM reductions may emerge over the course of development (van Amelsvoort et al. 2004). Although our findings are not entirely consistent with these results, this is not surprising given the differences in the age of the sample (children vs. adults) and study methodology (semiautomated voxel-based morphometry vs. cortical pattern matching).

In addition, consistent with the only existing large-scale study examining the relationship between IQ and cortical thickness (Shaw et al. 2006), we found a nonsignificant linear correlation between mean cortical thickness and IQ in our sample overall. In a sample of 307 healthy children and adolescents, Shaw et al. (2006) recently reported a complex relationship between development and cortical thickness; specifically, although there was an overall decline in cortical thickness throughout the age period studied, it was the trajectory of “change” in cortical thickness, rather than the thickness of the cortex itself, that showed the closest relationship with the level of intelligence. Unfortunately, this sort of complex, nonlinear relationship could not be examined in this cross-sectional study. Longitudinal studies are clearly warranted to better understand the effects of development on cortical alterations in this syndrome.

Candidate Genes for Cortical Dysmorphology in 22q11DS

Cortical architecture in 22q11DS is highly likely to be affected by haploinsufficiency for particular genes in the deleted region, but it is also likely to be dynamic, and environmental influences may also play a role (e.g., Simon et al. 2005). Although here we correlate a genetic mutation with anatomical change, direct causality cannot be determined; it is impossible to disentangle genetic and nongenetic influences as both may occur downstream of a genetic lesion. The observed cortical thinning may be shaped primarily by genetically programmed

anomalous neurodevelopment that impairs parietal-occipital structure and function. Several genes that influence neurogenesis and neuronal migration, including CRKL, zinc finger protein 74, platelet glycoprotein Ib, and its precursor, human cell division cycle-related protein-1 (peanut-like 1), are housed in the deleted 22q11.2 chromosomal region (Maynard et al. 2003), suggesting a possible genetic basis for the cortical dysmorphology observed here. In addition, the proline dehydrogenase (ProDH) gene, mapped to this region, regulates glutamate and γ -aminobutyrate (GABA) neurotransmission (Paterlini et al. 2005). ProDH-deficient mice have reduced glutamate, GABA, and aspartate levels in the hypothalamus and reduced GABA and aspartate in the frontal cortex (Gogos et al. 1999). Moreover, prepulse inhibition, a measure of sensorimotor gating, was decreased in these mice as compared with their littermates, a behavioral phenotype that has also been identified in children with 22q11DS (Sobin et al. 2005) and is associated with genetic risk for schizophrenia (Berrettini 2005). More recently, Mukai et al. (2004) also reported a significant association between a single nucleotide polymorphism in another gene in the 22q11 region, *ZDHHC8*, which is believed to be involved in palmitoylation, a process that modulates activity-dependent plasticity at glutamatergic synapses in the cortex and hippocampus (Jablensky 2004).

The embryological basis of the 22q11DS phenotype is believed to be aberrant cephalic neural crest migration to the third and fourth branchial arches (Marusich and Weston 1991) as many of the involved tissues (thymus, cardiac conotruncus, and parathyroid glands) are known to derive from the branchial arch/pharyngeal pouch system (Scambler 2000). This mechanism has yet to be confirmed, but experiments that perturb neural crest function can produce the main phenotypic features of 22q11DS; moreover, mutations of genes associated with neural crest development can similarly result in malformations that resemble those of 22q11DS (Roberts et al. 1997; Scambler 2000). Although it is tempting to hypothesize that the observed cortical thickness deficits may reflect a failure of neuronal migration in these brain regions, this possibility remains purely speculative at present.

Limitations

In this initial study, we did not attempt to recruit IQ-matched comparison subjects, resulting in a significant IQ difference between groups. The issue of appropriately matched comparison subjects is complex in developmentally delayed populations, given that individuals with comparable IQ to those with 22q11.2 deletions are likely to have intellectual disability of heterogeneous etiology, including undetected chromosomal abnormalities or unknown environmental exposures (e.g., lead exposure, fetal oxygen deprivation), which are likely to lead to a variety of cortical anomalies that are not well characterized. In addition, inclusion of children with familial low IQ and/or environmental exposures would likely lead to systematic “unmatching” on other demographic variables (i.e., parental education). As such, we adopted this more straightforward approach for our initial investigation but fully recognize that optimally designed future studies will include both normal as well as IQ-matched comparison groups.

Conclusions

This study provides novel information regarding localized thinning of the cortical mantle in children with 22q11.2 deletions. Our results point to a specific neuroanatomical basis for the visuospatial processing and visuomotor integration deficits observed in 22q11DS and suggest a possible mechanism by which regional cortical abnormalities may affect human visuospatial cognition. As the time course of cortical maturation is increasingly understood, the timing of the cortical anomaly in 22q11DS and the genetic cascades and gene-environment interactions that underlie it may be more completely elucidated.

Supplementary Material

Refer to Web version on PubMed Central for supplementary material.

Acknowledgments

Funding support for this work was provided in part by National Institute of Mental Health K23MH074644-01 (to CEB). Support for algorithm development was provided by the National Institute on Aging, the National Library of Medicine, the National Institute for Biomedical Imaging and Bioengineering, and the National Center for Research Resources (AG016570, LM05639, EB01651, RR019771 to PMT, P41 RR013642 to AWT).

References

- Ballmaier M, Kumar A, Thompson P, Narr K, Lavretsky H, Estanol L, Deluca H, Toga AW. Localizing gray matter deficits in late-onset depression using computational cortical pattern matching methods. *Am J Psychiatry* 2004;161(11):2091–2099. [PubMed: 15514411]
- Bearden CE, van Erp TG, Monterosso JR, Simon TJ, Glahn DC, Saleh PA, Hill NM, McDonald-McGinn DM, Zackai E, Emanuel BS, et al. Regional brain abnormalities in 22q11.2 deletion syndrome: association with cognitive abilities and behavioral symptoms. *Neurocase* 2004;10(3):198–206. [PubMed: 15788257]
- Bearden CE, Wang PP, Simon TJ. Williams syndrome cognitive profile also characterizes velocardiofacial/DiGeorge syndrome. *Am J Med Genet* 2002;114(6):689–692. [PubMed: 12210289]
- Bearden CE, Woodin MF, Wang PP, Moss E, McDonald-McGinn D, Zackai E, Emanuel B, Cannon TD. The neurocognitive phenotype of the 22q11.2 deletion syndrome: selective deficit in visual-spatial memory. *J Clin Exp Neuropsychol* 2001;23(4):447–464. [PubMed: 11780945]
- Berrettini WH. Genetic bases for endophenotypes in psychiatric disorders. *Dialogues Clin Neurosci* 2005;7(2):95–101. [PubMed: 16262206]
- Bingham PM, Zimmerman RA, McDonald-McGinn D, Driscoll D, Emanuel BS, Zackai E. Enlarged Sylvian fissures in infants with interstitial deletion of chromosome 22q11. *Am J Med Genet* 1997;74(5):538–543. [PubMed: 9342208]
- Chen CY, Zimmerman RA, Faro S, Parrish B, Wang Z, Bilaniuk LT, Chou TY. MR of the cerebral operculum: abnormal opercular formation in infants and children. *Am J Neuroradiol* 1996;17(7):1303–1311. [PubMed: 8871716]
- Chow EW, Zipursky RB, Mikulis DJ, Bassett AS. Structural brain abnormalities in patients with schizophrenia and 22q11 deletion syndrome. *Biol Psychiatry* 2002;51(3):208–215. [PubMed: 11839363]
- Cohen L, Dehaene S, Chochon F, Leherycy S, Naccache L. Language and calculation within the parietal lobe: a combined cognitive, anatomical and fMRI study. *Neuropsychologia* 2000;38(10):1426–1440. [PubMed: 10869586]
- Collins DL, Neelin P, Peters TM, Evans AC. Automatic 3D intersubject registration of MR volumetric data into standardized Talairach space. *J Comput Assist Tomogr* 1994;18(2):192–205. [PubMed: 8126267]
- Crow TJ. Temporal lobe asymmetries as the key to the etiology of schizophrenia. *Schizophr Bull* 1990;16(3):433–443. [PubMed: 2287933]
- Dapretto M, Bookheimer SY. Form and content: dissociating syntax and semantics in sentence comprehension. *Neuron* 1999;24(2):427–432. [PubMed: 10571235]
- Eliez S, Schmitt JE, White CD, Reiss AL. Children and adolescents with velocardiofacial syndrome: a volumetric MRI study. *Am J Psychiatry* 2000;157(3):409–415. [PubMed: 10698817]
- Eliez S, Schmitt JE, White CD, Wellis VG, Reiss AL. A quantitative MRI study of posterior fossa development in velocardiofacial syndrome. *Biol Psychiatry* 2001;49(6):540–546. [PubMed: 11257239]
- Evans, AC.; Collins, DL.; Holmes, CJ. Automatic 3D regional MRI segmentation and statistical probabilistic anatomical maps. New York: Academic Press; 1996.
- Flint J. The genetic basis of cognition. *Brain* 1999;122(Pt 11):2015–2032. [PubMed: 10545388]

- Galaburda AM, Geschwind N. Anatomical asymmetries in the adult and developing brain and their implications for function. *Adv Pediatr* 1981;28:271–292. [PubMed: 7041560]
- Galaburda AM, Sanides F, Geschwind N. Human brain. Cytoarchitectonic left-right asymmetries in the temporal speech region. *Arch Neurol* 1978;35(12):812–817. [PubMed: 718483]
- Gerdes M, Solot C, Wang PP, Moss E, LaRossa D, Randall P, Goldmuntz E, Clark BJ 3rd, Driscoll DA, Jawad A, et al. Cognitive and behavior profile of preschool children with chromosome 22q11.2 deletion. *Am J Med Genet* 1999;85(2):127–133. [PubMed: 10406665]
- Gogos JA, Santha M, Takacs Z, Beck KD, Luine V, Lucas LR, Nadler JV, Karayiorgou M. The gene encoding proline dehydrogenase modulates sensorimotor gating in mice. *Nat Genet* 1999;21(4):434–439. [PubMed: 10192398]
- Gogtay N, Giedd JN, Lusk L, Hayashi KM, Greenstein D, Vaituzis AC, Nugent TF 3rd, Herman DH, Clasen LS, Toga AW, et al. Dynamic mapping of human cortical development during childhood through early adulthood. *Proc Natl Acad Sci USA* 2004;101(21):8174–8179. [PubMed: 15148381]
- Harrison PJ. The neuropathology of schizophrenia. A critical review of the data and their interpretation. *Brain* 1999;122(Pt 4):593–624. [PubMed: 10219775]
- Highley JR, McDonald B, Walker MA, Esiri MM, Crow TJ. Schizophrenia and temporal lobe asymmetry. A post-mortem stereological study of tissue volume. *Br J Psychiatry* 1999;175:127–134. [PubMed: 10627794]
- Hubbard EM, Piazza M, Pinel P, Dehaene S. Interactions between number and space in parietal cortex. *Nat Rev Neurosci* 2005;6(6):435–448. [PubMed: 15928716]
- Jablensky A. Resolving schizophrenia's CATCH22. *Nat Genet* 2004;36(7):674–765. [PubMed: 15226748]
- Karmiloff-Smith A, Thomas M, Annaz D, Humphreys K, Ewing S, Brace N, Duuren M, Pike G, Grice S, Campbell R. Exploring the Williams syndrome face-processing debate: the importance of building developmental trajectories. *J Child Psychol Psychiatry* 2004;45(7):1258–1274. [PubMed: 15335346]
- Kates WR, Burnette CP, Jabs EW, Rutberg J, Murphy AM, Grados M, Geraghty M, Kaufmann WE, Pearlson GD. Regional cortical white matter reductions in velocardiofacial syndrome: a volumetric MRI analysis. *Biol Psychiatry* 2001;49(8):677–684. [PubMed: 11313035]
- Lu LH, Leonard CM, Thompson PM, Kan E, Jolley J, Welcome SE, Toga AW, Sowell ER. Normal developmental changes in inferior frontal gray matter are associated with improvement in phonological processing: a longitudinal MRI analysis. *Cereb Cortex*. 2006 June 6; 10.1093/cercor/bhl019.
- Luders E, Narr KL, Thompson PM, Rex DE, Jancke L, Toga AW. Hemispheric asymmetries in cortical thickness. *Cereb Cortex* 2006;16(8):1232–1238. [PubMed: 16267139]
- MacDonald D, Avis D, Evans A. Multiple surface identification and matching in magnetic resonance imaging. *Proc SPIE* 1994;2359:160–169.
- Marusich MF, Weston JA. Development of the neural crest. *Curr Opin Genet Dev* 1991;1(2):221–229. [PubMed: 1668308]
- Maynard TM, Haskell GT, Peters AZ, Sikich L, Lieberman JA, LaMantia AS. A comprehensive analysis of 22q11 gene expression in the developing and adult brain. *Proc Natl Acad Sci USA* 2003;100(24):14433–14438. [PubMed: 14614146]
- Mazziotta JC, Toga AW, Evans A, Fox P, Lancaster J. A probabilistic atlas of the human brain: theory and rationale for its development. The International Consortium for Brain Mapping (ICBM). *Neuroimage* 1995;2(2):89–101. [PubMed: 9343592]
- McDonald B, Highley JR, Walker MA, Herron BM, Cooper SJ, Esiri MM, Crow TJ. Anomalous asymmetry of fusiform and parahippocampal gyrus gray matter in schizophrenia: a postmortem study. *Am J Psychiatry* 2000;157(1):40–47. [PubMed: 10618011]
- McDonald-McGinn DM, LaRossa D, Goldmuntz E, Sullivan K, Eicher P, Gerdes M, Moss E, Wang P, Solot C, Schultz P, et al. The 22q11.2 deletion: screening, diagnostic workup, and outcome of results: report on 181 patients. *Genet Test* 1997;1(2):99–108. [PubMed: 10464633]
- Meyer-Lindenberg A, Mervis CB, Kippenhan JS, Olsen RK, Morris CA, Berman KF. Neural basis of genetically determined visuospatial construction deficit in Williams syndrome. *Neuron* 2004;43(5):623–631. [PubMed: 15339645]

- Milham MP, Nugent AC, Drevets WC, Dickstein DP, Leibenluft E, Ernst M, Charney D, Pine DS. Selective reduction in amygdala volume in pediatric anxiety disorders: a voxel-based morphometry investigation. *Biol Psychiatry* 2005;57(9):961–966. [PubMed: 15860335]
- Minier F, Carles D, Pelluard F, Alberti EM, Stern L, Saura R. [DiGeorge syndrome, a review of 52 patients]. *Arch Pediatr* 2005;12(3):254–257. [PubMed: 15734119]
- Moss EM, Batshaw ML, Solot CB, Gerdes M, McDonald-McGinn DM, Driscoll DA, Emanuel BS, Zackai EH, Wang PP. Psychoeducational profile of the 22q11.2 microdeletion: a complex pattern [see comments]. *J Pediatr* 1999;134(2):193–198. [PubMed: 9931529]
- Mukai J, Liu H, Burt RA, Swor DE, Lai WS, Karayiorgou M, Gogos JA. Evidence that the gene encoding ZDHC8 contributes to the risk of schizophrenia. *Nat Genet* 2004;36(7):725–731. [PubMed: 15184899]
- Murphy KC. Schizophrenia and velo-cardio-facial syndrome. *Lancet* 2002;359(9304):426–430. [PubMed: 11844533]
- O'Donnell S, Noseworthy MD, Levine B, Dennis M. Cortical thickness of the frontopolar area in typically developing children and adolescents. *Neuroimage* 2005;24(4):948–954. [PubMed: 15670671]
- Ono, M.; Kubik, S.; Abernathy, C. Atlas of the cerebral sulci. Stuttgart (Germany): Thieme; 1990.
- Paterlini M, Zakharenko SS, Lai WS, Qin J, Zhang H, Mukai J, Westphal KG, Olivier B, Sulzer D, Pavlidis P, et al. Transcriptional and behavioral interaction between 22q11.2 orthologs modulates schizophrenia-related phenotypes in mice. *Nat Neurosci* 2005;8(11):1586–1594. [PubMed: 16234811]
- Reiss AL, Abrams MT, Singer HS, Ross JL, Denckla MB. A volumetric imaging study. Brain development, gender and IQ in children. *Brain* 1996;119(Pt 5):1763–1774. [PubMed: 8931596]
- Roberts C, Daw SC, Halford S, Scambler PJ. Cloning and developmental expression analysis of chick Hira (Chira), a candidate gene for DiGeorge syndrome. *Hum Mol Genet* 1997;6(2):237–245. [PubMed: 9063744]
- Scambler PJ. The 22q11 deletion syndromes. *Hum Mol Genet* 2000;9(16):2421–2426. [PubMed: 11005797]
- Shattuck DW, Leahy RM. BrainSuite: an automated cortical surface identification tool. *Med Image Anal* 2002;6(2):129–142. [PubMed: 12045000]
- Shaw P, Greenstein D, Lerch J, Clasen L, Lenroot R, Gogtay N, Evans A, Rapoport J, Giedd J. Intellectual ability and cortical development in children and adolescents. *Nature* 2006;440(7084):676–679. [PubMed: 16572172]
- Simon T, Bearden C, Moss E, Zackai E, Wang P. Cognitive development in velocardiofacial syndrome. *Prog Pediatr Cardiol* 2002;15(2):109–117.
- Simon T, Bish J, Bearden C, Ding L, Ferrante S, Nguyen V, Gee J, McDonald-McGinn D, Zackai E, Emanuel BS. A multiple levels analysis of cognitive dysfunction and psychopathology associated with chromosome 22q11.2 deletion syndrome in children. *Dev Psychopathol* 2005;17(3):753–784. [PubMed: 16262991]
- Sobin C, Kiley-Brabeck K, Karayiorgou M. Associations between prepulse inhibition and executive visual attention in children with the 22q11 deletion syndrome. *Mol Psychiatry* 2005;10(6):553–562. [PubMed: 15520831]
- Sowell ER, Thompson PM, Holmes CJ, Jernigan TL, Toga AW. In vivo evidence for post-adolescent brain maturation in frontal and striatal regions. *Nat Neurosci* 1999;2(10):859–861. [PubMed: 10491602]
- Sowell ER, Thompson PM, Tessner KD, Toga AW. Mapping continued brain growth and gray matter density reduction in dorsal frontal cortex: inverse relationships during postadolescent brain maturation. *J Neurosci* 2001;21(22):8819–8829. [PubMed: 11698594]
- Sun T, Patoine C, Abu-Khalil A, Visvader J, Sum E, Cherry TJ, Orkin SH, Geschwind DH, Walsh CA. Early asymmetry of gene transcription in embryonic human left and right cerebral cortex. *Science* 2005;308(5729):1794–1798. [PubMed: 15894532]
- Swillen A, Devriendt K, Legius E, Prinzie P, Vogels A, Ghesquiere P, Fryns JP. The behavioural phenotype in velo-cardio-facial syndrome (VCFS): from infancy to adolescence. *Genet Couns* 1999;10(1):79–88. [PubMed: 10191433]

- Thompson PM, Hayashi KM, de Zubicaray G, Janke AL, Rose SE, Semple J, Herman D, Hong MS, Dittmer SS, Doddrell DM, et al. Dynamics of gray matter loss in Alzheimer's disease. *J Neurosci* 2003;23(3):994–1005. [PubMed: 12574429]
- Thompson PM, Hayashi KM, Sowell ER, Gogtay N, Giedd JN, Rapoport JL, de Zubicaray GI, Janke AL, Rose SE, Semple J, et al. Mapping cortical change in Alzheimer's disease, brain development, and schizophrenia. *Neuroimage* 2004;23:S2–S18. [PubMed: 15501091]
- Thompson PM, Lee AD, Dutton RA, Geaga JA, Hayashi KM, Eckert MA, Bellugi U, Galaburda AM, Korenberg JR, Mills DL, et al. Abnormal cortical complexity and thickness profiles mapped in Williams syndrome. *J Neurosci* 2005;25(16):4146–4158. [PubMed: 15843618]
- Thompson PM, Vidal C, Giedd JN, Gochman P, Blumenthal J, Nicolson R, Toga AW, Rapoport JL. Mapping adolescent brain change reveals dynamic wave of accelerated gray matter loss in very early-onset schizophrenia. *Proc Natl Acad Sci USA* 2001;98(20):11650–11655. [PubMed: 11573002]
- van Amelsvoort T, Daly E, Henry J, Robertson D, Ng V, Owen M, Murphy KC, Murphy DG. Brain anatomy in adults with velocardiofacial syndrome with and without schizophrenia: preliminary results of a structural magnetic resonance imaging study. *Arch Gen Psychiatry* 2004;61(11):1085–1096. [PubMed: 15520356]
- van Amelsvoort T, Daly E, Robertson D, Suckling J, Ng V, Critchley H, Owen MJ, Henry J, Murphy KC, Murphy DG. Structural brain abnormalities associated with deletion at chromosome 22q11: quantitative neuroimaging study of adults with velo-cardio-facial syndrome. *Br J Psychiatry* 2001;178:412–419. [PubMed: 11331556]
- Woodin M, Wang PP, Aleman D, McDonald-McGinn D, Zackai E, Moss E. Neuropsychological profile of children and adolescents with the 22q11.2 microdeletion. *Genet Med* 2001;3(1):34–39. [PubMed: 11339375]
- Wright I, Rabe-Hesketh S, Woodruff P, David A, Murray R, Bullmore E. Meta-analysis of regional brain volumes in schizophrenia. *Am J Psychiatry* 2000;157:16–25. [PubMed: 10618008]

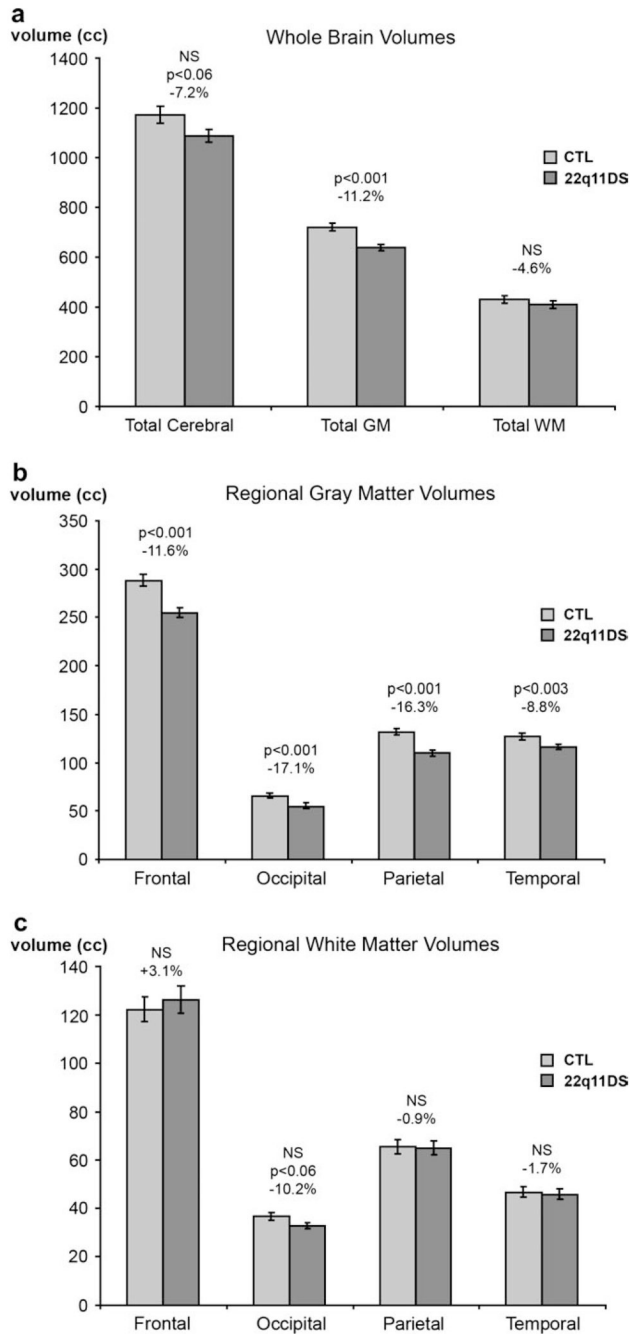


Figure 1. Comparison of brain volumes in children with 22q11DS and healthy controls. Means and standard error measures (error bars) are shown for (a) overall cerebral GM and WM, (b) lobar WM, and (c) lobar GM. Children with 22q11DS show significant GM decreases in all lobes but only a trend toward WM volume reduction in occipital cortex.

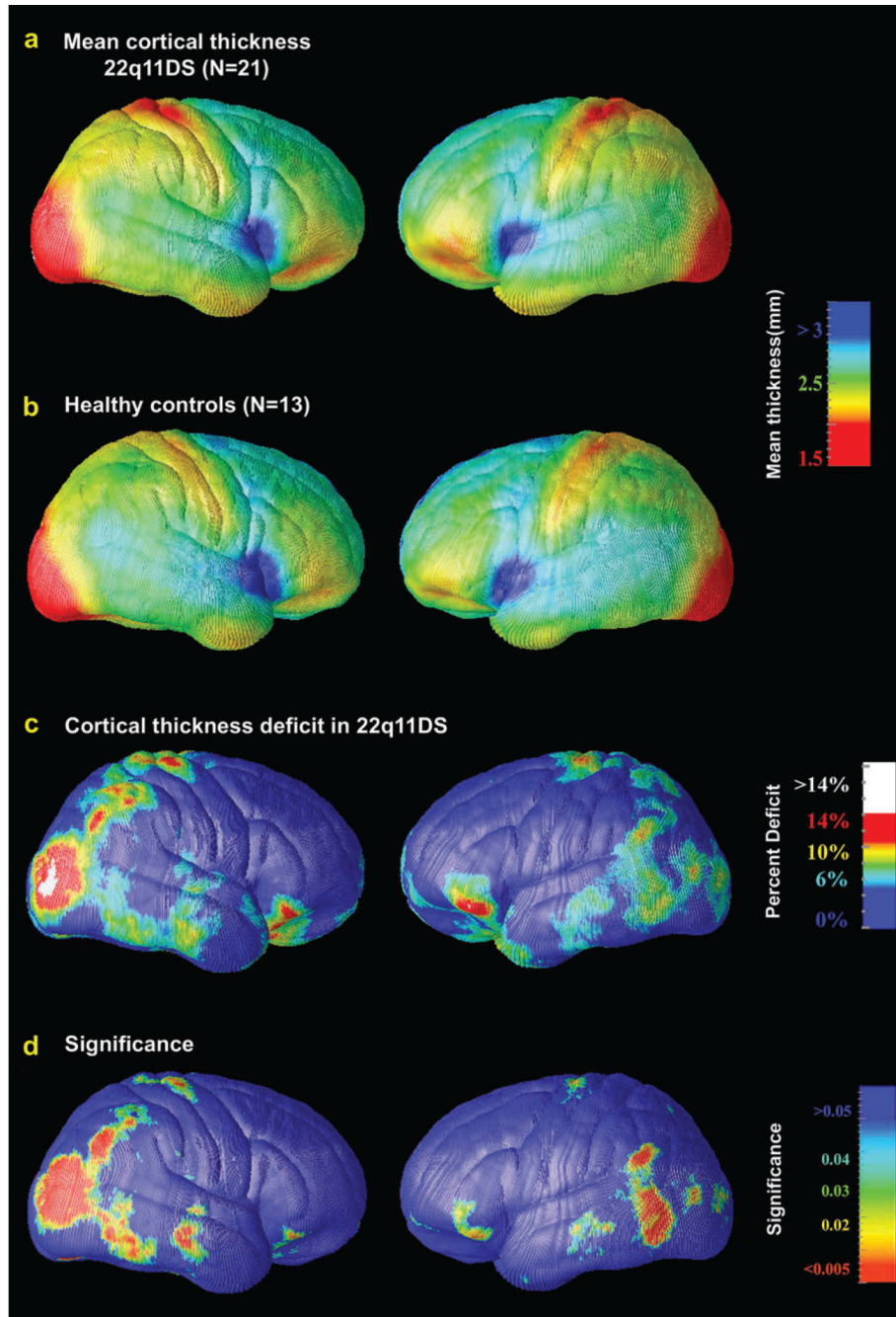


Figure 2. Cortical thickness maps: regional decreases in 22q11DS. The mean thickness maps for 22q11DS subjects (*a*, $N = 21$) and controls (*b*, $N = 13$) are shown, on a color-coded scale where blue colors denote thicker cortex, red colors thinner cortex. Thickness is in millimeters, according to the color bar (values are not scaled and represent estimates of the true thickness in each subject). As evident in (*a*) and (*b*), there is remarkable similarity between the regional thickness patterns in the 2 groups. The mean decrease in cortical thickness in 22q11DS is shown as a percentage of the control average in (*c*). Red colors, in parietooccipital cortex and the inferior-most portion of the IFG (pars orbitalis) and lateral orbital gyrus, denote regions that are up to 14% thinner, on average, than corresponding areas in controls. In the RH, greater

than 14% reduction in cortical thickness was observed in an area encompassing the lateral occipital gyrus (shown in white). Blue colors denote regions where the thickness was the same or higher in 22q11DS. A previous finding by Eliez et al. (2000) indicating reduced parietal lobule volume in 22q11DS, even after adjusting for differences in brain volume, is consistent with the thinning of parietal cortex seen here. The significance of these reductions is plotted in (d) as a map of P values.

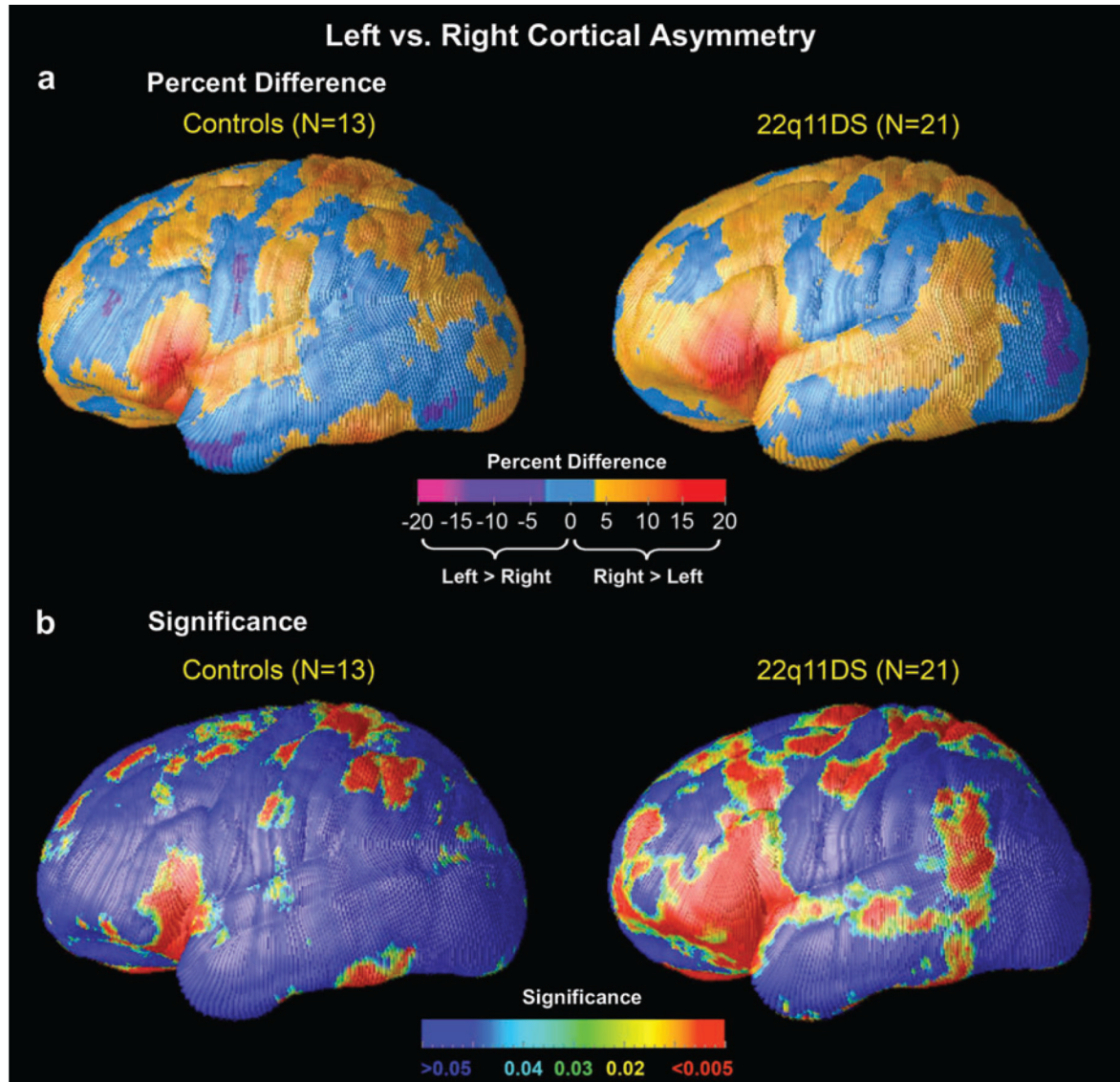


Figure 3.

Cortical asymmetry maps. (a) Maps of cortical thickness asymmetry expressed as a percentage, for control subjects (top left panel) and 22q11DS (top right panel). Negative values on the color bar (purple and magenta) encode a greater thickness in the LH (i.e., leftward asymmetry), whereas positive values (orange and red) represent greater thickness in the RH (i.e., rightward asymmetry). (b) Depicts uncorrected maps of significant cortical thickness asymmetry, in controls (bottom left panel) and 22q11DS (bottom right panel). The color bar encodes the P value associated with the t -tests of cortical thickness performed at each cortical surface point. All blue-shaded regions are not significantly different between LH and RH. Measures of asymmetry are shown on one hemisphere only as they are, by definition, the same for both hemispheres. Rightward ($R > L$) asymmetries of cortical thickness were of greatest magnitude in the IFG in both 22q11DS and control children but were more extensive in the brains of 22q11DS participants (a and b, right panel).

Table 1

Demographics of 22q11DS and comparison subjects

	22q11DS subjects (N = 21)	Comparison subjects (N = 13)	P value
Age (\pm SD)	11.7 (\pm 2.82)	10.9 (\pm 2.63)	$F_{1,32} = 0.68, P = 0.42$
Sex			$\chi^2_{34} = 0.13, P = 0.72$
Male	10 (48%)	7 (54%)	
Female	11 (52%)	6 (46%)	
Race (% Caucasian)	100%	100%	$\chi^2_{34} = 0.00, P = 1.0$
Handedness (% right)	20 (95%)	12 (92%)	$\chi^2_{34} = 0.27, P = 0.61$
Parental education (\pm SD)	15.2 (\pm 2.7)	15.1 (\pm 2.7)	$F_{1,32} = 0.03, P = 0.89$
Verbal IQ (\pm SD)*	78.6 (\pm 15.6)	111.0 (\pm 14.3)	$F_{1,32} = 34.5, P < 0.001$
Performance IQ (\pm SD)*	73.2 (\pm 12.6)	109.1 (\pm 10.9)	$F_{1,32} = 67.5, P < 0.001$
Full-scale IQ (\pm SD)*	74.5 (\pm 14.6)	111.3 (\pm 12.3)	$F_{1,32} = 54.7, P < 0.001$
DSM-IV psychiatric diagnoses ^a			
No diagnosis	9 (43%)		
ADHD	6 (28.6%)		
Oppositional defiant disorder	1 (4.8%)		
PDD/psychosis NOS	1 (4.8%)		
Anxiety disorders	10 (47.6%)		
Specific phobia	4 (19%)		
Social phobia/GAD	1 (4.8%)		
OCD traits	2 (9%)		
PTSD/acute stress disorder	1 (4.8%)		
Panic disorder	1 (4.8%)		
Anxiety disorder NOS	1 (4.8%)		

Note: SD, standard deviation; ADHD, attention deficit hyperactivity disorder; PDD, pervasive developmental disorder; NOS, not otherwise specified; GAD, generalized anxiety disorder; OCD, obsessive compulsive disorder; PTST, posttraumatic stress disorder.

^aSome patients have more than one diagnosis.

* $P \leq .01$